NOAA Technical Report NESDIS 31

Data Processing Algorithms for Inferring Stratospheric Gas Concentrations from Balloon-Based Solar Occultation Data

Washington, D.C.
April 1987

U.S. DEPARTMENT OF COMMERCE
National Oceanic and Atmospheric Administration
National Environmental Satellite, Data, and Information Service

NOAA TECHNICAL REPORTS

National Environmental Satellite, Data, and Information Service

The National Environmental Satellite, Data, and Information Service (NESDIS) manages the Nation's civil operational Earth-observing satellite systems, as well as global national data bases for meteorology, oceanography, geophysics, and solar-terrestrial sciences. From these sources, it develops and disseminates environmental data and information products critical to the protection of life and property, national defense, the national economy, energy development and distribution, global food supplies, and the development of natural resources.

Publication in the NOAA Technical Report series does not preclude later publication in scientific journals in expanded or modified form. The NESDIS series of NOAA Technical Reports is a continuation of the former NESS and EDIS series of NOAA Technical Reports and the NESC and EDS series of Environmental Science Services Administration (ESSA) Technical Reports.

These reports are available from the National Technical Information Service (NTIS), U.S. Department of Commerce, Sills Bldg., 5285 Port Royal Road, Springfield, VA 22161. Prices on request for paper copies or microfiche.

A more complete listing of these reports, by title and NTIS accession number, is available from the Assessment and Information Services Center, National Oceanic and Atmospheric Administration, Code E/AI13, Page Bldg. 2, 3300 Whitehaven Street, N.W., Washington, DC 20235. A partial listing of more recent reports appears below:

NESS Series

NESS 89 A Statistical Approach to Rainfall Estimation Using Satellite and Conventional Data. Linwood F. Whitney, Jr. April 1982. (PB82 215435)

NESS 90 Total Precipitable Water and Rainfall Determinations From the SEASAT Scanning Multichannel Microwave Radiometer (SMMR). John C. Alishouse, May 1982. (PB83 138263)

NESS 91 Numerical Smoothing and Differentiation by Finite Differences. Henry E. Fleming and Lawrence J. Crone, May 1982. (PB82-258385)

NESS 92 Satellite Infrared Observations of Oceanic Long Waves in the Eastern Equatorial Pacific 1975 to 1981. Richard Legeckis, November 1982. (PB83 161133)

NESS 93 A Method for Improving the Estimation of Conditional Instability from Satellite Retrievals. W.E. Togstad, J.M. Lewis, and H.M. Woolf, November 1982. (PB83 169938)

EDIS Series

EDS 29 GATE Convection Subprogram Data Center: Final Report on Rawinsonde Data Validation. Robert W. Reeves, March 1978. (PB-281-861)

EDS 30 Gamma Distribution Bias and Confidence Limits. Harold L. Crutcher and Raymond L. Joiner, September 1978. (PB-289-721)

EDIS 31 Calibration and Intercomparison of the GATE C-Band Radars. M. Hudlow, R. Arkell, V. Patterson, P. Pytlowany, F. Richards, and S. Geotis (MIT), November 1979. (PB81 120305)

EDIS 32 Distribution of Radiosonde Errors. Harold L. Crutcher, May 1979. (PB-297-383)

EDIS 33 Accurate Least-Squares Techniques Using the Orthogonal Function Approach. Jerry Sullivan, March 1980. (PB80 223241)

EDIS 34 An Application of Stochastic Forecasting to Monthly Averaged 700 mb Heights. Albert Koscielny, June 1982. (PB82 244625)

NESDIS Series

NESDIS 1 Satellite Observations on Variations in Southern Hemisphere Snow Cover. Kenneth F. Dewey and Richard Heim, Jr., June 1983. (PB83 252908)

NESDIS 2 NODC 1 An Environmental Guide to Ocean Thermal Energy Conversion (OTEC) Operations in the Gulf of Mexico. National Oceanographic Data Center (DOC/NOAA Interagency Agreement Number EX-76-A-29-1041), June 1983. (PB84 115146)

NESDIS 3 Determination of the Planetary Radiation Budget From TIROS-N Satellites. Arnold Gruber, Irwin Ruff, and Charles Earnest, August 1983. (PB84 100916)

NESDIS 4 Some Applications of Satellite Radiation Observations to Climate Studies. T. S. Chen, George Ohring, and Haim Ganot, September 1983. (PB84 108109)

NESDIS 5 A Statistical Technique for Forecasting Severe Weather From Vertical Soundings by Satellite and Radiosonde. David L. Keller and William L. Smith, June 1983. (PB84 114099)

(Continued on inside back cover)

NOAA Technical Report NESDIS 31

Data Processing Algorithms for Inferring Stratospheric Gas Concentrations from Balloon-Based Solar Occultation Data

I-Lok Chang
American University
Washington, D.C. 20016

Michael P. Weinreb
Satellite Research Laboratory
National Environmental Satellite, Data,
and Information Service
Washington, D.C.

April 1987

U.S. DEPARTMENT OF COMMERCE
Malcolm Baldrige, Secretary

National Oceanic and Atmospheric Administration
Anthony J. Calio, Under Secretary

National Environmental Satellite, Data, and Information Service
Thomas N. Pyke, Assistant Administrator

CONTENTS

FIGURES

DATA PROCESSING ALGORITHMS FOR INFERRING STRATOSPHERIC GAS CONCENTRATIONS FROM BALLOON-BASED SOLAR OCCULTATION DATA

I-Lok Chang
The American University
Washington, D.C. 20016

Michael P. Weinreb
National Oceanic and Atmospheric Administration
National Environmental Satellite, Data, and Information Service
Washington, D.C. 20233

ABSTRACT. In three high-altitude balloon experiments, we inferred concentrations of ozone, water vapor, and other gases in the stratosphere, using the technique of solar occultation. Our objective was to demonstrate feasibility of a new technique before implementing it on a satellite, and to gain experience with handling the data. This technical report documents fully and in detail the methods we developed for processing the data. It presents the equations that describe the atmospheric physics of the measurement and the algorithms to solve them. It also presents practical aspects of applying the algorithms to real data, methods for overcoming aberations and problems inherent in the occultation technique, and sample results.

1. INTRODUCTION

A series of balloon-based solar occultation experiments have been conducted by the NOAA National Environmental Satellite, Data, and Information Service. The main objective of the experiments was to investigate the feasibility of using a multi-detector grating spectrometer to sense trace constituents in the stratosphere by measuring solar absorption. This report presents the data processing and the computational aspects of the experiments. Specifically, we describe the formulation of the retrieval equations, the reduction of the front-end data, and the computations performed to invert the equations to obtain constituent profiles. As a part of our attempt to make this report as self-contained as possible, we give a brief sketch of the instrumentation. We must point out, however, that several physical and mathematical formulations we used have been fully explained and presented in journals and books. For their derivations, we shall refer the readers to their sources.

2. INSTRUMENTATION

The instrument is described in Weinreb et al. (1984). In brief, it is a multi-detector grating spectrometer that detects radiation continuously in a number of discrete infrared spectral intervals (channels), six of which are described in Table 1. They are located in the absorption bands of HNO_3, CF_2Cl_2, O_3 and H_2O. Radiation was focussed onto the spectrometer by a telescope that provided an angular field of view of 8 arc minutes. A system of motors was incorporated to point the instrument at the sun.

TABLE 1. Spectral Intervals for Balloon Spectrometer

Interval	Central Wavenumber (cm^{-1})	Half-Power Bandwidth (cm^{-1})	Species
1	886	5	Nitric acid
2	930	4	Freon-12
3	980	6	Ozone, low altitude
4	998	3	Ozone, high altitude
5	1507.0	3	Water vapor, high altitude
6	1528.5	4.5	Water vapor, low altitude

3. MATHEMATICAL FORMULATIONS

3.1 Geometry of the Experiment and Formulation of Retrieval Procedures

In June 1982 a balloon carried the instruments to the altitude of 39 km over Palestine, Texas. The system collected occultation data for several hours until sunset. The next experiment took place in April 1983, at an altitude of 42 km. The final experiment was conducted in July 1985, from an altitude of 39 km. From high sun to sunset, the spectrometer system tracked the sun, taking solar intensity data at a rate of 20 times per second in each channel. During the experiment, radiation from the sun passed through the atmosphere in a curved refracted path, and entered the instrument, where it was dispersed and detected in the six channels. In each channel, a sequence of solar intensities was measured, from the beginning to the end of the experiment.

To designate a ray, we call the point on the ray path that is closest to the center of the earth the tangent point of the ray. The altitude of the tangent point is called the tangent height. The angle formed by the radial line to the balloon and a ray that reaches the balloon is called the solar zenith angle of the ray. Figure 1 shows a ray with its tangent point, tangent height, and its solar zenith angle.

For analysis of the data, we picture the atmosphere divided into spherical layers which are concentric with the earth. Altogether we used thirty-eight concentric layers. The part of the atmosphere of interest is the range within the stratosphere from 10 km to 46 km. This portion contains thirty-six equally spaced layers, with radial spacing of 1 km. The atmosphere above 46 km and the portion below 10 km are the two remaining layers (see Figure 1). Starting from the top layer (45 km-46 km) and proceeding downward, the 37 boundary spherical shells that separate the layers are denoted as the first shell, the second shell, . . ., the kth shell,..., and the 37th shell.

In each experiment, the calculation that inverted the measured solar intensities into a set of concentration profiles took the form of solving a system of nonlinear equations,

$$\tau_i(C_1, C_2, \ldots, C_N) + \varepsilon_i = t_i, \quad i=1,2,\ldots,K. \tag{1}$$

The function τ_i in each equation is a theoretical transmittance function, ε_i is an error term, and the right-hand quantity t_i is a transmittance derived from the measured solar intensities as we shall describe in section 4. The unknowns $C_1, C_2, \ldots, C_N$ are concentrations (or mixing ratios) of one or several species at the boundary shells, indexed according to some scheme related to the indices of the boundary shells. Each equation represents a ray that enters the spectrometer, defined by its tangent height. Every equation is simply a statement that the concentrations $C_1, C_2, \ldots, C_N$ along the path of the ray should yield a (theoretically predicted) transmittance τ_i equalling the measured transmittance t_i--to within an uncertainty of ε_i.

Each experiment lasted several hours, as the sun was tracked from a high-sun position to sunset. The portion of data we selected for retrieval typically began with a solar zenith angle of about 85° and concluded with an angle of about 96°. We call the period from the occurrence of a 90° solar zenith angle to the end of the experiment the occultation period. Transmittances measured within the occultation period in general contained significantly more information than those measured at earlier times of the experiment. We call the transmittances measured during the occultation period "total transmittances", and those before the occultation period "outer transmittances". We use "outer" in the sense that the observed ray traversed only the portion of the atmosphere above the balloon level. In a typical system of retrieval equations described in (1), the majority of the equations were equations of total transmittances, i.e., t_i of such an equation was a "total transmittance". The remaining equations were equations of "outer transmittances".

A set of rays were chosen to provide the transmittances t_i. During each experiment, the balloon drifted slowly, ascending and descending within an altitude range of 1.1 km. For the "total transmittances", we chose the sequence of ray paths which were tangent to the boundary shells, from the balloon height downward. For the "outer transmittances", we chose those ray paths whose geometric extensions beyond the balloon were tangential to the boundary shells (see Figure 2). Thus each ray path provided a transmittance t_i for one equation in the system (1). The geometric characteristics of the path, the atmospheric data, and the estimated concentrations C_j along the path constituted the input for the theoretical transmittance function τ_i in the equation.

Each transmittance function τ_i calculates the transmittance along the path of a selected ray. Because of the need for a fast algorithm to compute such forward transmittances, we have adopted a simplified occultation model for computing τ_i. The simplification here concerns the gradual vertical and lateral drift of the balloon during an experiment. Taking into account the balloon motion introduces several complications into the "forward" computation of the transmittances $\tau_1, \ldots, \tau_K$. In all three experiments, the vertical drift was always within 1 km of a boundary shell. In the experiments of 1982 and 1985, the balloon moved about the altitude of 39 km. In 1983, it moved gradually up and down about 42 km. For all the experiments, one can estimate easily and show that two rays that enter the balloon instrument from the same tangent height but with a change in the balloon altitude of 1 km differ in their transmittances by an amount significantly smaller than the expected error contributed by other sources in the experiment. The same conclusion is valid also for the changes in the transmittance functions introduced by the lateral drift of the balloon. Based on this observation, in each experiment, we determined a "mean balloon position". The point always remained fixed on a chosen boundary shell. Whenever a forward transmittance τ_i for a ray with a designated tangent height was to be computed, the balloon would first be "moved" to the fixed position. A slightly altered ray path with the same tangent height would then be used to compute the transmittance τ_i. Thus the spatial setting for each retrieval calculation took the form of a balloon that remained fixed on a boundary shell, observing rays from the sun as it descended into the horizon.

3.2 The Geometric Zenith Angle: Calculation and Usage

We now describe a parameter that played an important role in the processing of the balloon data. In reducing the data to obtain a set of transmittances $t_1, \ldots, t_K$, we used the angle θ shown in Figure 3 to locate the rays that

were to provide the transmittances. We call this angle the geometric solar zenith angle of a ray. The angle is the angular span between the radial line passing through the balloon and the straight line joining the balloon and the sun. In each experiment, in the first stage of data reduction, we began by naming a set of tangent heights whose rays would be the sources of the transmittances $\{t_i\}$. We then performed a search in the data set to locate a block of rays for each tangent height. Each block would contain data for rays whose tangent heights clustered about the chosen tangent height. Now, the data set of each experiment comprised a sequence of "ray records". Each record contained the information and measurements for a ray. To locate a cluster of rays about a tangent height, we first determined the value that has to be assumed by the geometric solar zenith angle θ_{th} ("th" for "tangent height") for a ray in order that the actual refracted ray be tangent to the chosen tangent height. Then starting at an appropriate point in the data set, we examined the "ray records" one by one. At each record, we computed the corresponding geometric solar zenith angle θ_{ray} for the ray. The angle θ_{ray} was computed from the time of the observation and the ephemeris of the sun. If θ_{ray} matched θ_{th}--to within a matching tolerance, we considered the search for the rays about the current chosen tangent height completed. We proceeded to compute a set of average transmittances, over a block of rays about the current ray. One average transmittance was computed for each channel, thus obtaining six average transmittances for the tangent height, to be used as t_i's in various systems of retrieval equations.

In computing the angle θ_{th}, we employed a ray-trace method together with simple interpolation schemes. A derivation of the ray-trace method can be found in Watson and Yin (1973). The method computes the geometric zenith angle θ of a ray with a specified tangent height and at a specified balloon position. We sketch here the steps involved in the case of a ray with a tangent height below the balloon height--a ray that yields a total transmittance. For a ray that yields an outer transmittance, the steps are similar. From Figure 3, the angle θ can be expressed as

$$\theta = \phi + \omega ,$$

where ϕ is the true zenith angle of the ray, which includes the influence of refraction by the atmosphere. The angle of refraction is ω. The angle ϕ can be determined from the refraction equation

$$n_1 r_1 \sin \phi = n_o r_o , \qquad (2)$$

where r_o is the radial distance from the tangent point to the center of the

earth, r_1 is the radial distance of the balloon, n_o and n_1 are the indices of refraction at the points where the ray intersects r_o and r_1 respectively. A basic assumption we made in this series of experiments was that the atmosphere was spherically symmetric. With this assumption, the refraction index n(r) of the atmosphere is a function of the radial distance r only. For n(r) we used the equation $n(r) = 1 + C\,(P(r)/T(r))$, generating interpolated values for the pressure value P(r) and the temperature value T(r) whenever necessary. For the constant C, we used the value $C = 77.5 \times 10^{-6}$ °K/mb, obtained from The Handbook of Geophysics (1960). The angle ω can be calculated from n(r) with two integrals

$$\omega = \frac{2}{n_o r_o} \int_0^1 \frac{r\,(-dn/dr)}{(r^{-1} + n^{-1}\,dn/dr)}\,dY + \frac{2}{n_o r_o} \int_0^{Y_b} \frac{r\,(-dn/dr)}{(r^{-1} + n^{-1}\,dn/dr)}\,dY \quad . \tag{3}$$

The variable of integration is $Y = \cos\psi$, where ψ is the supplement of the zenith angle at a point on the path of the refracted ray (see Figure 3). The upper limit Y_b in the second integral is $\cos(\pi-\phi)$. The first integral represents the refraction between the sun and the tangent point; the second the refraction between the tangent point and the balloon. In the quadrature algorithms we adopted for evaluating the integrals, we used finite differences for the values of dn/dr. As an example of a computed geometric zenith angle, in the experiment of April 1983, with the balloon at the altitude of 42 km, we found that the ray tangent to the balloon height had a geometric solar zenith angle of 90 degrees and 0.06 minute, and the ray with the tangent height of 26 km had a geometric zenith angle of 94 degrees and 4.58 minutes. In the first case, the ray tangent to the balloon position had undergone a refraction of 0.06 minute. The true zenith angle was of course 90 degrees.

We must point out that, unlike the forward computation of the transmittance function τ_i, the calculation of the geometric zenith angle θ_{th} of a tangent height must retain the balloon height as a variable, for the vertical drift of the balloon can now affect the computed value of θ_{th} in a significant way. The argument we give for keeping the balloon fixed on a boundary shell when computing τ_i is no longer applicable for the computation of θ_{th} if the balloon drift can be as high as 1 km. For example, in the experiment of 1983, the balloon ascended from 40.8 km to 41.9 km during the experiment. Suppose that we wish to locate in the data set the part that contains the rays with tangent

heights in the range of 28 km. In calculating the angle θ_{th}, if we assume a fixed balloon height of 41 km, where the actual height is 41.9 km, then the matching method we used may yield a ray whose actual tangent height is above 28 km. Similarly, if the zenith angle θ_{th} is calculated with a fixed balloon altitude higher than the actual balloon height, the matching ray may have an actual tangent height that is below 28 km. For this experiment, in the tangent-height range of 10 km to 30 km, an error of 1 km in balloon altitude used for computing θ_{th} can result in selecting a ray whose actual tangent height can be 0.9 km either above or below the intended tangent height. The resulting errors in the derived transmittances can be larger than the 0.01 error tolerance which we have imposed for this series of experiments. For this reason, in the experiments of 1983 and 1985, the computation of θ_{th} required computing its value from the actual balloon height at each "ray record". As the number of "ray records" examined in each experiment was of the order of 17,000 records, we have used interpolation of θ_{th} on the balloon heigh to alleviate the computation of θ_{th}. This will be explained more fully in section 4.1 .

We shall stop at this point our general description of the experiments. We have presented aspects of the experimental setting, theoretical formulations, data processing schemes, and the various assumptions we made to simplify the retrieval calculation. We now proceed to describe in a more detailed manner the conversion of balloon data into the transmittances $t_1,\ldots,t_K$.

4. FRONT-END PROCESSING OF THE BALLOON DATA

4.1 Reduction of Balloon Data to Transmittances

In the flight experiment, the data were recorded on tape. In each experiment, data in all channels were sampled 20 times in each second. We shall call the set of data in one sample a record. The data were transferred from the tape to a "front-end" file in the NOAA central computer facility, and at the same time some preliminary processing was carried out. The data from the spectrometer and from "housekeeping" sensors were calibrated from counts to voltage outputs. In the case of the measurement of atmospheric pressure, the voltages were converted to units of atmosphere pressure through a calibration determined just before the balloon launch. Then we derived the balloon altitude by logarithmic interpolation in a table of altitude versus pressure provided after the flight by the NOAA/Climate Analysis Center (M. Gelman, personal communication, 1983, 1985). The temperature of each of the six detectors, also monitored, was derived from a pre-launch calibration. On the computer file, each record contained the data of one ray:

hour and minute in central daylight time,
balloon height in kilometers,
six channels of voltages to be converted into transmittances,
six detector temperatures.

In each experiment, a set of tangent heights were selected to provide transmittances for the retrieval calculation. Proceeding from the upper stratosphere downward, the tangent heights were selected with a vertical spacing of 1 km. For the experiment of June 1982, total transmittances were determined for the tangent heights 39 km, 38 km, . . . , 22 km. In the experiment of April 1983, we were able to obtain total transmittances from 42 km to 22 km, and outer transmittances from 22 km to 42 km (tangent height of an outer transmittance is the tangent height of the extended ray). For the experiment of July 1985, total transmittances were measured from 36 km to 12 km, and outer transmittances from 17 km to 26 km. In that experiment, because of two short periods of data loss at the beginning of the experiment, we used polynomial interpolation to infer the total transmittances from 38 km to 36 km, and outer transmittances from 27 km to 39 km.

The procedure for derivation of the transmittances of the designated tangent heights followed the search-and-average method described in the previous section (section 3.2). For instance, in the experiment of 1983, to determine the total transmittances, we started with the search for the ray with a tangent height which was closest to the first designated tangent height, 42 km. Starting from a point in the data set shortly before occultation period began, the data were examined record by record. At each record, the required geometric zenith angle for a ray to have a tangent height of 42 km was first determined as described previously. Then the actual geometric zenith angle from the balloon at that moment was calculated (the angle θ_{ray}). To calculate the latter zenith angle, first we calculated the latitude and the longitude of the balloon using simple polynomial interpolation, interpolating in time within a balloon trajectory provided by National Scientific Balloon Facility at Palestine, Texas. From time, latitude, and longitude, the zenith angle was then calculated using ephemeris equations and ephemeris data obtained from The American Ephemeris and Nautical Almanac (1981, 1982, and 1984). The two zenith angles were then compared. When an acceptable match in the two angles had been found, a block of rays with the current ray at its center was then marked for averaging. The length of the block was 30 rays for the first experiment, and 170 rays for the next two experiments. Within the block, the voltages of the six channels were first converted to transmittances using calibration schemes described in the next section. The transmittances in each channels were then averaged to obtain a value representing the measured transmittance for the channel at the tangent height. After the average transmittances had been determined, the search then continued to locate the next block of data for the next tangent height.

In determining the maximum block length of 170 rays for averaging, the basic consideration was to avoid having vertical smearing over an extent large compared to the instrument field of view. In each experiment, the vertical

view of the telescope was 8.5 arc minutes, and the center of the field of view moved approximately at a rate of 0.25 arc minute per second. At a data rate of 20/sec, the smearing resulting from 170 rays was approximately only 1/4 of the vertical field of view.

The method we employed to calculate the geometric solar zenith angle θ_{th} for a tangent height varied with the experimental conditions. If the vertical drift of the balloon was not significant, the angles θ_{th} of all designated tangent heights were calculated only once, at the beginning of the search, with the balloon fixed at the altitude chosen for calculating the forward transmittances τ_i (see section 3.1). If the drift in balloon altitude was not negligible, the angle θ_{th} of a designated tangent height was calculated at each "ray record", as the records were examined one by one. Such repeated calculation of the geometric solar zenith angle of a tangent height was performed with the data of the experiments of 1983 and 1985. We implemented a polynomial interpolation scheme for such computation. As an example, in 1983, the balloon ascended from 40.8 km to 41.9 km during the period of the experiment. First we set up a table that contained four sets of geometric zenith angles, one set each for the balloon altitudes of 42 , 41.5 , 41 and 40.5 km, respectively. Each set is a column of geometric zenith angles computed as a function of the tangent heights of the boundary shells, from the balloon level downward to the level of 23 km. The angles were calculated using the equations in (2) and (3), as we discussed in section 3.2. We saved the resulting table of angles in a two dimensional array. After computing the table, the linear search then commenced. When searching in the data set for a ray for a specified tangent height, at each "ray record", the balloon height at the moment served as the independent variable for interpolating a zenith angle θ_{th} from among the angles in the table. The interpolation polynomials were cubic hermite polynomials. We found the method stable and satisfactory.

In the 1985 experiment, there was an additional complexity. Because of difficulties with the system for pointing the instrument at the sun, the field of view slowly oscillated vertically on the face of the sun. As a result, the zenith angle θ_{ray} did not increase monotonically with time, and there could be more than one time when $\theta_{th} = \theta_{ray}$. Therefore, to guarantee that the best possible time was chosen, we inspected computer print-outs of the data. In the procedure, the assumption that θ_{ray} , the zenith angle of the line of sight, equaled the zenith angle of the center of the sun was no longer true, and a correction had to be made for the deviation. The angular correction was evaluated from signals from a pair of detectors in the telescope, which monitored the location of the field of view on the sun's surface.

The procedures we have described above served as the basic procedures for the front-end processing to obtain a set of transmittances from the data set. Various correction or selection schemes were added at different points to make

adjustments to the data. For instance, all voltage spikes in the six spectral channels were rejected, and in the third experiment, at periods where data loss occurred, cubic hermite polynomials were used to provide interpolated transmittances.

4.2 Calibration Methods

We transformed the voltages measured during the occultation period to transmittances by dividing them by the 100% signals, i.e., the signals that would be measured in the absence of any atmosphere. In channels 1, 2, and 6, the atmospheric absorption was so weak that the signals measured before sunset, when the solar zenith angle was relatively small, were essentially the 100% signals. However, in the other channels this was not the case, and direct measurement of the 100% signal was impossible. In these channels, we used two different techniques to find the 100% signals. For the 1982 experiment, we used the relation

$$N(i) = N(2)\ [G(i)/G(2)][S(i)/S(2)],$$

where N is the unattenuated signal (expressed in volts), i the interval number, G the gain of the instrument (output volts/input radiance), and S the solar radiance. The quantity N(2), the unattenuated signal in interval 2, was measured during the flight. The values of G were measured in tests conducted in a vacuum chamber before the fligt. The ratios of the solar radiance were taken from the literature (Thekaekara, 1971). Interval 2 was used as the basis for this procedure because it is the interval in which the upper atmosphere absorbs the least. The validity of this technique depended on the assumption that G(i)/G(2) was invariant over the time interval between the pre-flight vacuum tests and the flight. Although the assumption appeared to be valid for the 1982 flight, we had some evidence in the 1983 and 1985 flights that it was not. Therefore, for the latter two experiments, we inferred the 100% signals by extrapolating back to zero airmass the signals measured before the solar zenith angle reached 90°. Figure 4 shows an example of the procedure. The data in this figure are from the 1985 experiment before the solar zenith angle reached 90°. The abscissa is airmass, which is represented by the length of the path between the balloon and the altitude of 50 km, above which it is assumed that there is no absorption. The signal for zero airmass is derived from the y-intercept. For example, in channel 4, the intercept is 1.567. Thus the zero-path signal is 4.792 volts.

5. RETRIEVAL CALCULATION

5.1 The Transmittance Equations

We now describe the transmittance equations (1) in a more detailed manner. The aim of solving the system of equations was to determine an approximation

to the vertical concentration profile (or mixing ratio profile) of each of the constituents: ozone, water vapor, nitric acid, and Freon-12. The set of concentrations { C_1, C_2, . . ., C_N } in each system of equations consisted of either the concentrations of a single species at a set of selected boundary shells, or the concentrations of two species, in the case of nitric acid and Freon-12, at a set of boundary shells. Each equation seldom involved the complete set of concentrations from C_1 to C_N. The concentrations $\{C_j\}$ that appeared in each equation were only those that contributed to the absorption along the ray path.

The "measured" transmittances t_1, ... , t_K in each system of equations were either the outer transmittances and the total transmittances computed by the front-end program, or the values from the front-end program with further modification to take into account of the absorption by other species of molecules. For the water vapor retrieval, each t_i was furthered divided by a transmittance to correct for the absorption due to molecular oxygen (Shapiro and Gush, 1966). In the retrieval of nitric acid and Freon-12, the absorption due to carbon dioxide was accounted for in the same way, by dividing each t_i by the carbon dioxide transmittance that had been computed once and for all in advance (Weinreb and Chang, 1987).

The function τ_i is a theoretical transmittance function that yields a transmittance for a ray that passes through a specified tangent height and arrives at the balloon. We refer to Weinreb et al. (1984), and Weinreb and Chang (1987), for a detailed discussion of the formulation of the transmittance functions. In each calculation of τ_i, the necessary atmospheric data (pressures, temperatures) were obtained from the height-temperature profiles provided by Mr. Melvyn E. Gelman of NOAA's Climate Analysis Center.

The term ε_i is an error term that includes experimental errors and approximation errors in the calculation of τ_i. Studies of sources of error in the experiments can be found in Weinreb et al. (1984) and Weinreb and Chang (1987).

A complete system of equations, with outer and total transmittances, and usually with t_i measured in two channels, is a conglomerate of transmittance equations of various types. For instance, in a water vapor retrieval calculation for the 1985 experiment, the entire system consisted of fourteen outer transmittance equations for channel 5 (26 km to 39 km), twenty-four outer transmittance equations for channel 6 (16 km to 39 km), twenty-eight total transmittance equations for channel 5 (39 km to 12 km), and twenty-eight total transmittance equations for channel 6 (39 km to 12 km). With C_1, C_2, .

. . . , C_{35} denoting the concentrations of water vapor at 46 km, 45 km, . . ., 12 km respectively, the equations were sequenced in the following order,

outer transmittances channel 5

$$\tau_1(C_1,\ldots,C_8) + \varepsilon_1 = t_1$$

$$\vdots$$

$$\tau_{14}(C_1,\ldots,C_8) + \varepsilon_{14} = t_{14}$$

outer transmittances channel 6

$$\tau_{15}(C_1,\ldots,C_8) + \varepsilon_{15} = t_{15}$$

$$\vdots$$

$$\tau_{38}(C_1,\ldots,C_8) + \varepsilon_{38} = t_{38}$$

total transmittances channel 5

$$\tau_{39}(C_1,\ldots,C_8) + \varepsilon_{39} = t_{39}$$

$$\vdots$$

$$\tau_{66}(C_1,\ldots,C_{35}) + \varepsilon_{66} = t_{66}$$

total transmittances channel 6

$$\tau_{67}(C_1,\ldots,C_8) + \varepsilon_{67} = t_{67}$$

$$\vdots$$

$$\tau_{94}(C_1,\ldots,C_{35}) + \varepsilon_{94} = t_{94}$$

Altogether the system contained ninety-four equations with thirty-five unknowns.

In some retrieval calculations, the number of unknown concentrations exceeded the number of equations. Such a system usually has infinitely many solutions, all satisfying the equations. For instance, in the experiment of 1982, no outer transmittance was calculated from the data. In determining an approximate water vapor concentration profile that only channel 6 alone would yield, the available transmittance equations were the equations of 39 km, 38 km, . . ., 24 km--a total of sixteen equations. The concentrations to be determined were those from the top level of 46 km to the level of 24 km--a total of twenty-three concentrations. In such a situation, in order to avoid having numerous unrealistic but mathematically correct solutions, we always reduced the number of unknowns by keeping the concentrations above the balloon level constant, fixed at a guessed profile, thus achieving equality in the number of unknowns and the number of equations. A discussion of the sensitivity of a retrieved profile to errors in the guessed concentration profile at the upper levels can be found in Chang and Weinreb (1985).

The procedure just described of using a fixed partial profile is a way of resolving the problem of not having enough transmittance information above the balloon level for retrieving the concentration profile in that range. We present here another method to eliminate the concentrations above the balloon level from the transmittance equations. The method is still in the testing stage, requiring further numerical results to confirm its numerical stability. From Figure 5, observe that with the assumption of spherical symmetry, the outer transmittance of ray A is also the partial transmittance of ray B along the outer portion of the ray from the balloon level to the sun. If we divide the total transmittance t_i of ray B by the outer transmittance from ray A, and assuming multiplicative law of transmittance, then the transmittance equation of ray B now involves only the concentrations from the balloon level downward. The necessary corresponding modification in each equation in (1) is simply to change the calculation of each τ_i from integrating from the balloon to the sun to integrating only along the portion of ray B within the boundary shell of the balloon. One advantage of this method is that we have eliminated in each equation the portion of the concentration profile which is most susceptible to noise in transmittance data in a retrieval calculation. Computationally, fewer steps are required to obtain a concentration profile because of the reduction in the number of unknowns. This method is described in more detail in Weinreb and Chang (1987).

5.2 Retrieval Algorithms

The retrieval equations in the system (1) are nonlinear equations. We inverted the system using an iterative scheme. The method is a simple Levenberg-Marquardt algorithm. Let $\underline{t}$ denote the column vector of

transmittances $t_1, t_2, \ldots, t_K$, $\underline{\tau}$ the column vector of transmittance functions $\tau_1, \tau_2, \ldots, \tau_K$, and $\underline{C}$ the column vectors of concentrations $C_1, C_2, \ldots, C_N$. Starting from an initial estimate $\underline{C}^{(0)}$, the method generates a sequence of concentration profiles $\underline{C}^{(1)}, \underline{C}^{(2)}, \ldots, \underline{C}^{(i)}, \underline{C}^{(i+1)}, \ldots$, to minimize $Q(\underline{C}) = \| \underline{\tau}(\underline{C}) - \underline{t} \|^2$, where $\| \underline{\tau}(\underline{C}) - \underline{t} \|$ denotes the length of the vector $\underline{\tau}(\underline{C}) - \underline{t}$. The vectorial function $\underline{\tau}(\underline{C}) - \underline{t}$ is a non-linear function of $\underline{C}$. The iterative minimization of its length is based on the local Taylor expansion of $\underline{\tau}(\underline{C})$ in terms of $\underline{C}$. Specifically, in the ith iteration ($i \geq 0$), having obtained $\underline{C}^{(i)}$ from the previous step, the Taylor expansion of $\underline{\tau}(\underline{C})$ has the form

$$\underline{\tau}(\underline{C}) = \underline{\tau}^{(i)} + J^{(i)} (\underline{C} - \underline{C}^{(i)}) + \ldots , \qquad (4)$$

where $\underline{\tau}^{(i)} = \underline{\tau}(\underline{C}^{(i)})$, $J^{(i)}$ is the Jacobian matrix $\{\partial \tau_m / \partial C_n\}$ evaluated at $\underline{C}^{(i)}$. The first two terms of the series gives a simple first-order approximation of $\underline{\tau}(\underline{C})$. Using this approximation, the next step in the algorithm is to minimize the following quadratic form:

$$Q^{(i)} = \| \underline{\tau}^{(i)} + J^{(i)}(\underline{C} - \underline{C}^{(i)}) - \underline{t} \|^2 + \lambda^2 \| \underline{C} - \underline{C}^{(i)} \|^2 , \qquad (5)$$

where λ is a parameter to restrict the range of $\underline{C}$ in the minimization of $Q^{(i)}$. In application, λ is usually called a smoothing parameter. Minimizing $Q^{(i)}$ is equivalent to solving the linear least squares problem

$$\begin{bmatrix} J^{(i)} \\ \lambda I_N \end{bmatrix} (\underline{C} - \underline{C}^{(i)}) \cong \begin{bmatrix} \underline{t} - \underline{\tau}^{(i)} \\ \underline{0}_N \end{bmatrix} \qquad (6)$$

in which N is the number of variables in $\underline{C}$, I_N is the NxN identity matrix and $\underline{0}_N$ is a column of N zeros. We computed $J^{(i)}$ using finite-difference schemes in most cases, and using analytic partial derivatives of $\underline{\tau}$ whenever they were

available. To solve equation (6), we employed a method of singular-value decomposition. The method is described in Lawson and Hanson (1974), pp. 190-192. Briefly, the method begins with a singular-value decomposition of $J^{(i)}$. (For simplicity, we shall suppress many of the indices i, the iteration index). The decomposition of the Jacobian matrix has the form

$$J = USV^T$$

where J is a KxN matrix, U a KxK orthogonal matrix, V an NxN orthogonal matrix, and S a KxN matrix with N singular values along its main diagonal,

$$\begin{bmatrix} \sigma_1 & & & \\ & \sigma_2 & & 0 \\ & & \ddots & \\ 0 & & & \sigma_N \\ & & 0 & \end{bmatrix} \qquad (K \geq N) .$$

The singular values $\sigma_1, \ldots, \sigma_N$ are ordered in decreasing magnitudes, i.e.,

$$\sigma_1 \geq \sigma_2 \geq \ldots \geq \sigma_N \geq 0.$$

Let n be the number of non-zero singular values. Define the vector

$$(a_1, \ldots, a_K)^T = U^T[\underline{t} - \underline{\tau}(\underline{c}^{(i)})].$$

Now compute the vector $\underline{y}$ whose elements are given by

$$y_j = \begin{cases} a_j \sigma_j / (\sigma_j^2 + \lambda^2) & \text{for } j \leq n \\ 0 & \text{for } n < j \leq N \end{cases}$$

Then the solution of (6) is given by

$$\underline{c}^{(i+1)} = \underline{c}^{(i)} + V\,\underline{y}$$

The parameter λ is an auxiliary parameter for controlling the size of the step $\Delta\underline{c}$,

$$\Delta\underline{c} = \underline{c}^{(i+1)} - \underline{c}^{(i)} .$$

The length of $\Delta\underline{c}$ can be expressed as

$$L(\lambda) = \| \Delta\underline{c} \| = \left[\sum_{j=1}^{n} (a_j/\sigma_j)^2 (\sigma_j^2/(\sigma_j^2 + \lambda^2))^2 \right]^{1/2}$$

Without λ in equations (5) and (6)--by choosing $\lambda = 0$, we are minimizing $Q^{(i)} = \| \underline{\tau}^{(i)} + J^{(i)}(\underline{c} - \underline{c}^{(i)}) - \underline{t} \|$ with a step length of $L(0)$. If λ is positive, the step length taken is always less than the full length, i.e., $L(\lambda) < L(0)$. In this case, it can be shown that $\underline{c}^{(i+1)}$ is the solution to the minimization problem,

$$\min \| \underline{\tau}^{(i)} + J^{(i)}(\underline{c} - \underline{c}^{(i)}) - \underline{t} \|^2 ,$$

where $\underline{c}$ is restricted to the spherical neighborhood $\| \underline{c} - \underline{c}^{(i)} \| \leq L(\lambda)$. (See Dennis and Schnabel, 1983, Chapter 10.) Thus λ constrains the search of for the minimum of

$$\| \underline{\tau}^{(i)} + J^{(i)}(\underline{c} - \underline{c}^{(i)}) - \underline{t} \|^2 \approx \| \underline{\tau}(\underline{c}) - \underline{t} \|^2$$

to a smaller region about $\underline{c}^{(i)}$. We found that a full step almost always moved $\underline{c}$ so far from $\underline{c}^{(i)}$ that the Taylor approximation was no longer accurate. A full step usually led to an increase instead of decrease in $\| \underline{\tau}(\underline{c}) - \underline{t} \|^2$, even though $Q^{(i)}$ was minimized. We used in each retrieval a fixed λ, usually

of one or two orders of magnitude less than σ_1, the largest singular value of $J^{(i)}$. We found no more than six iterations were usually necessary to reduce $\| \underline{\tau}(\underline{C}) - \underline{t} \|$ to achieve

$$| \tau_i(\underline{C}) - t_i | \leq 0.01 \quad ,$$

$i = 1, 2, \ldots, K$, where 0.01 was approximately the level of instrument noise.

It is not difficult to see that constraining the step size $\| \Delta \underline{C} \|$ to a small magnitude also contributes to maintaining the smoothness of the retrieved profile, for the step-by-step change from a smooth initial profile is performed in a gradual manner. Occasionally we have used other strategies provided by the Levenberg-Marquardt algorithm to affect the shape of the retrieved profile in order to conform to additional boundary conditions. A discussion of such methods can be found in Chang and Weinreb (1985), pp. 159-160.

We have presented retrieval results in Weinreb et al., (1984, 1986, 1987), Chang and Weinreb (1985), Weinreb and Chang (1985). We show here a set of retrieved profiles from the experiment of 1985. In Figure 6, a retrieved ozone mixing ratio profile is compared with concurrent measurements obtained from balloon-borne electrochemical concentration cells. In Figure 7, a retrieved water vapor mixing ratio profile is compared with in-situ frost-point hygrometer measurements. The concurrent measurements for both ozone and water vapor were provided by S. Oltman of the National Oceanic and Atmospheric Administration, Environmental Research Laboratories. A retrieved nitric acid mixing ratio profile is given in Figure 8, superimposed with profiles measured in previous years by other investigators (see WMO, 1982). A retrieved Freon-12 mixing ratio profile is presented in Figure 9, alongside an envelope constructed from previous measurements (WMO, 1982), by projecting prior measurements to 1985 with an assumed growth rate of 5% per year. In this figure, the tropopause height is 15 km for the retrieved profile and 13 km for the prior measurements. Detailed analysis of this group of retrieval results can be found in Weinreb and Chang (1987).

6. CONCLUSION

We have presented procedures we used for processing infrared solar occultation measurements to infer trace gas mixing ratios in the stratosphere. The basis of the procedures is a system of equations that describes the atmospheric physics of the measurements. We have described a matrix algorithm for solving the equations, and have presented some sample results. However, the emphasis of this report has been on the practical aspects of working with real data and the various irregularities. Thus, we presented geometric

concepts such as inference of tangent height from time of observation (including refraction effects). We also described the calibration of the raw data to the "measured" atmospheric transmittances, and methods for compensating for instrument problems. Because of its practical emphasis, this report should be useful as a manual to aid scientists in designing processing systems for occultation measurements.

REFERENCES

Chang, I-Lok, M.P. Weinreb, 1985: Retrieval calculations applied to solar occultation measurements. Advances in Remote Sensing Retrieval Methods, edited by A. Deepak, H.E. Fleming, and M.T. Chahine, published by A. Deepak Publishing, Hampton, VA, 149-163.

Dennis, J.E., Jr., and P.B. Schnabel, 1983. Numerical Methods for Unconstrained Optimization and Nonlinear Equations. Prentice Hall, Inc., Englewood Cliff, N. J., 378 pp.

Handbook of Geophysics, 1980, Revised Ed. (Macmillan, New York), Chap. 3.

Gelman, M.E. (National Oceanic and Atmospheric Administration, Climate Analysis Center, U.S. Department of Commerce, Washington, D.C.), 1983, 1985 (personal communications).

Lawson, C.L., and R.J. Hanson, 1974. Solving Least Squares Problems. Prentice Hall, Inc., Englewood Cliff, N.J., 378 pp.

The American Ephemeris and Nautical Almanac. U.S. Government Printing Office, Washington, D.C., 20402, 1981, 1982, and 1984.

Thekaekara, M.P., 1971(second printing - 1973): Solar electromagnetic radiation. NASA SP-8005, Goddard Space Flight Center, Greenbelt, MD, 37 pp.

Shapiro, M.M. and H.P. Gush, 1966: The collision-induced fundamental and first overtone bands of oxygen and nitrogen. Can. J. Phys. 44, 949-963.

Watson, J.K.G. and P.K.L. Yin, 1973: The effects of refraction and dispersion on high-altitude measuremnets of atmospheric gases. Interim Report, NOAA grant NG-28-72, The Ohio State University Research Foundation, Columbus, Ohio, 100 pp.

Weinreb, M.P., W.A. Morgan, I-Lok Chang, L.D. Johnson, P.A. Bridges, and A.C. Neuendorffer, 1984: High-altitude balloon test of satellite solar occultation instrument for monitoring stratospheric O_3, H_2O and HNO_3. Journal of Atmospheric and Oceanic Technology, Vol. 1, No. 1, 87-100.

Weinreb, M.P. and I-Lok Chang, 1985: Effect of Absorption by the upper atmosphere in balloon-based solar occultation experiments. A paper presented at Amer. Meteor. Soc., 5th Conf. on Meteorology of the Stratosphere and Mesosphere, Boulder, CO, April 23-26, 1985.

Weinreb, M.P., L.J. Johnson, P.A. Bridges, M.L. Hill, I-Lok Chang, S. Oltmans, A. Sanyal, and W. A. Morgan, 1986: Balloon-based solar occultation measurements of stratospheric constituent profiles. A paper presented at Amer. Meteor. Soc., 2nd Conf. on Satellite Remote Sensing and Applications, Williamsburg, VA, May 13-16, 1986.

Weinreb, M.P. and I-Lok Chang, 1987: Balloon-based infrared solar occultation measurements of stratospheric O_3, H_2O, HNO_3, and CF_2Cl_2. Submitted to J. Geophys. Res..

World Meteorological Organization, The stratosphere 1981: theory and measurements, WMO Global Ozone Res. Monitoring Proj. Rep. No. 11, Geneva, 1982.

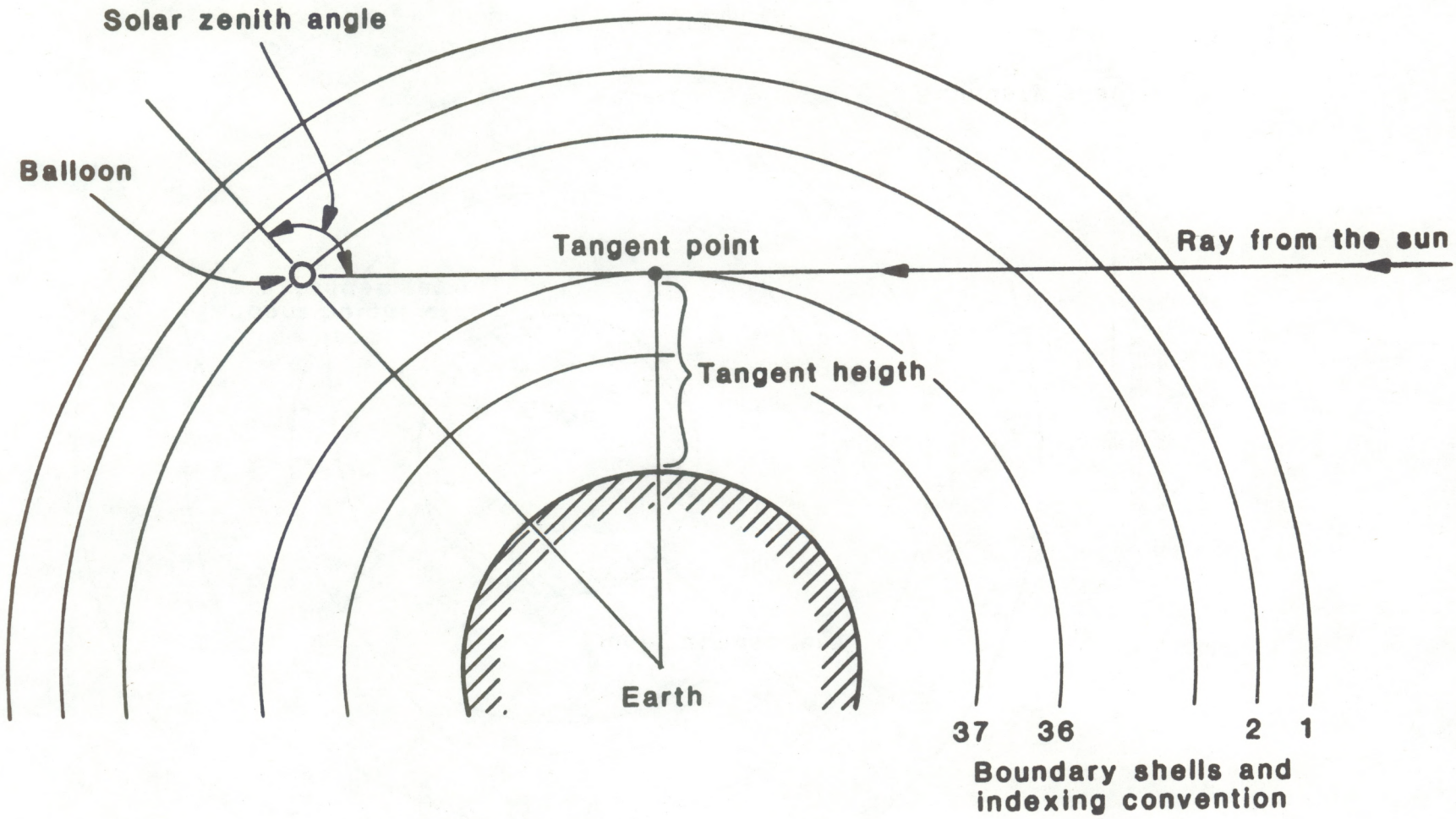

Figure 1. Solar occultation geometry.

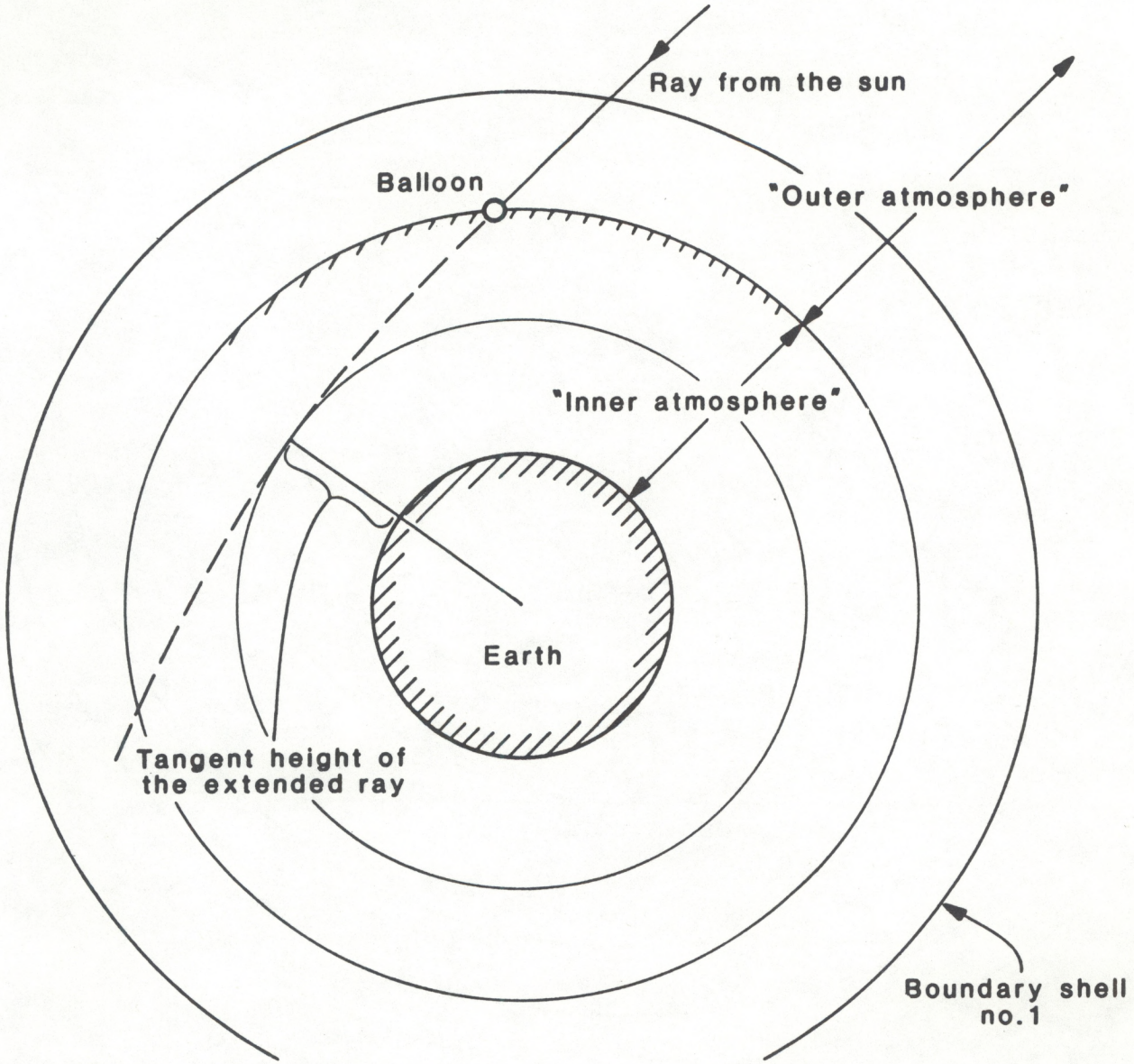

Figure 2. Geometry of "outer-transmittance".

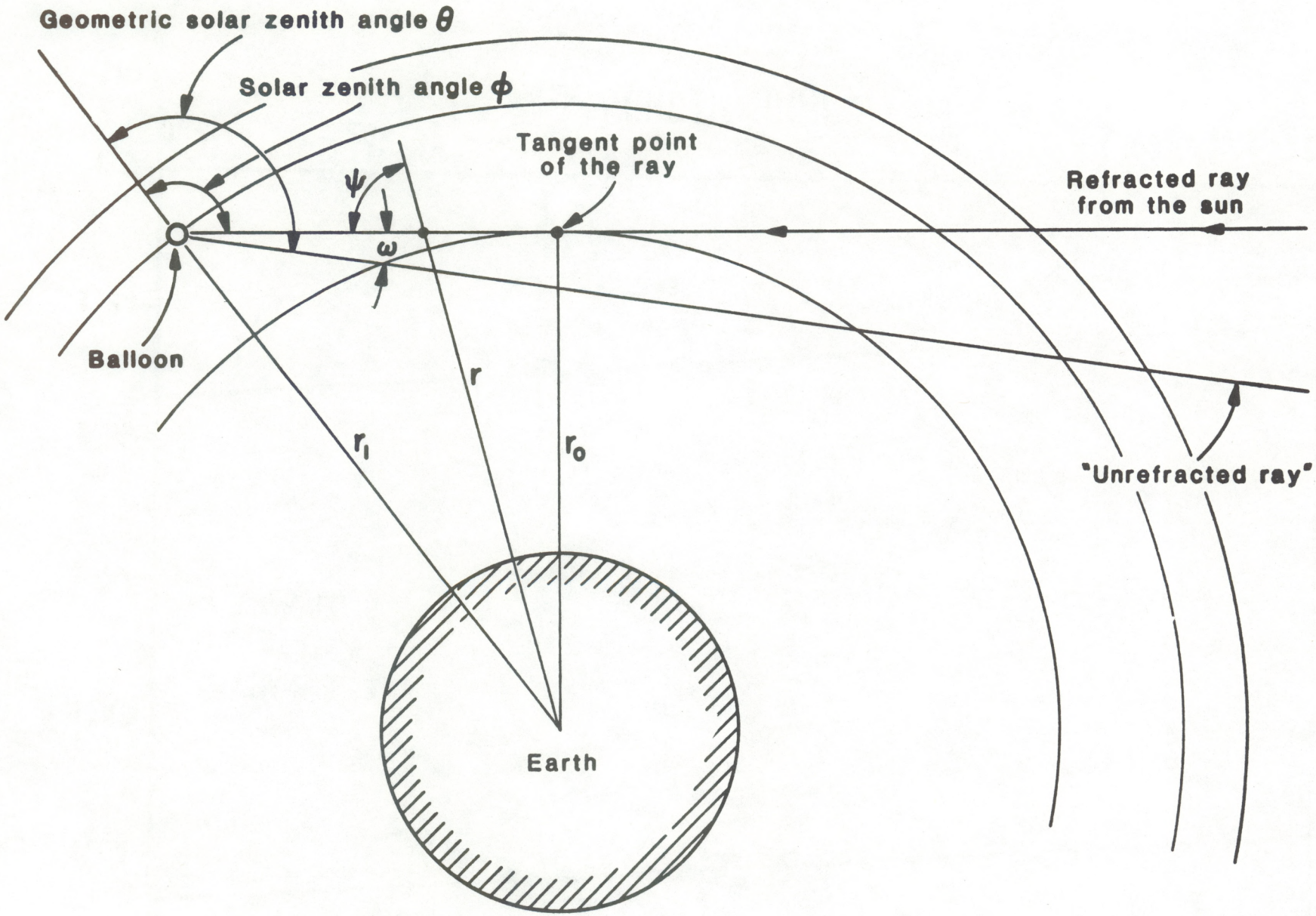

Figure 3. Parameters associated with a refracted ray and parameters used to describe the corresponding "unrefracted ray".

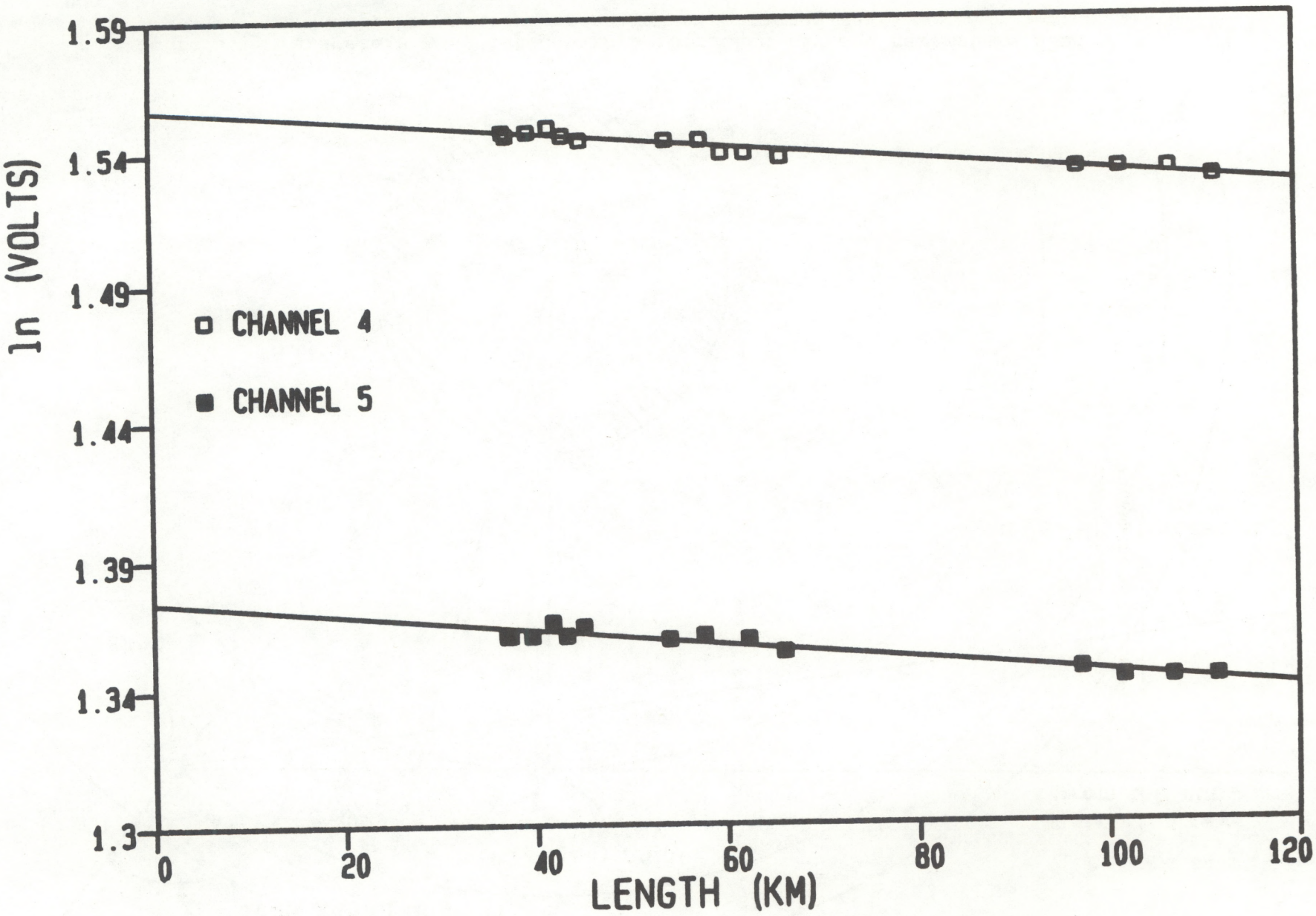

Figure 4. Example of extrapolation of signals to zero path length.

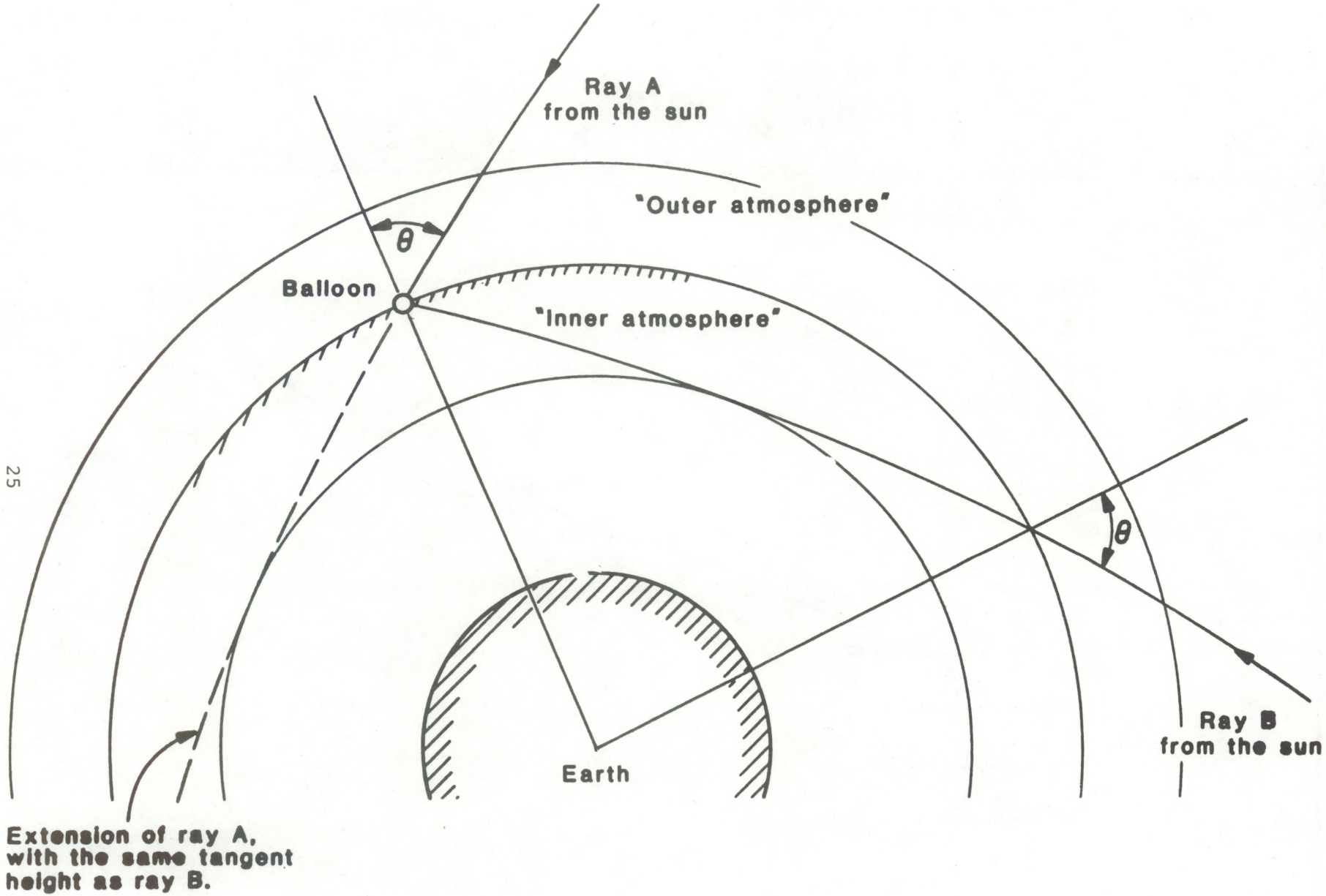

Figure 5. Geometry for removal of the effect of "outer atmosphere" in retrieval calculation.

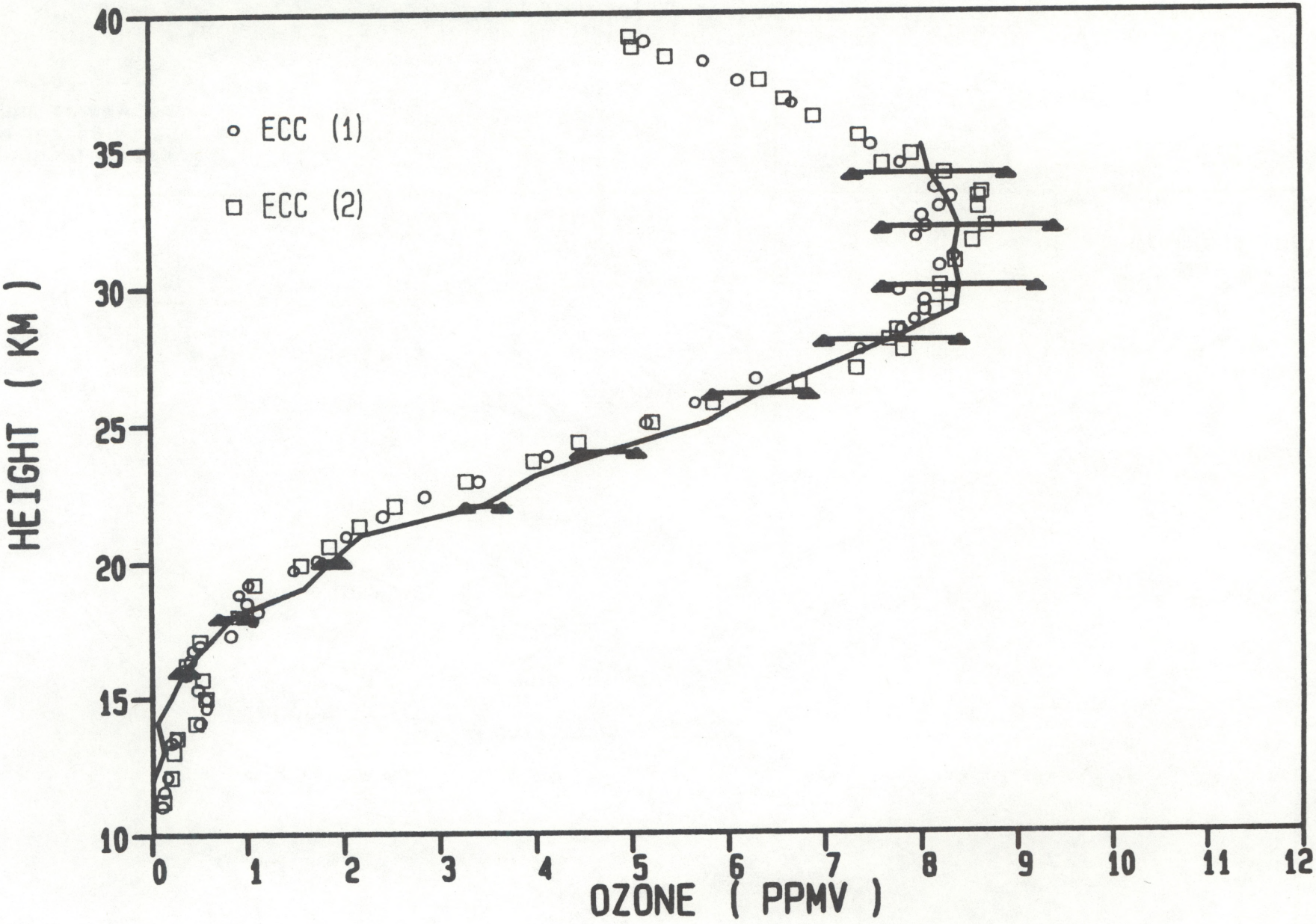

Figure 6. Retrieved ozone mixing ratio profile and concurrent ECC measurements from 1985 experiment.

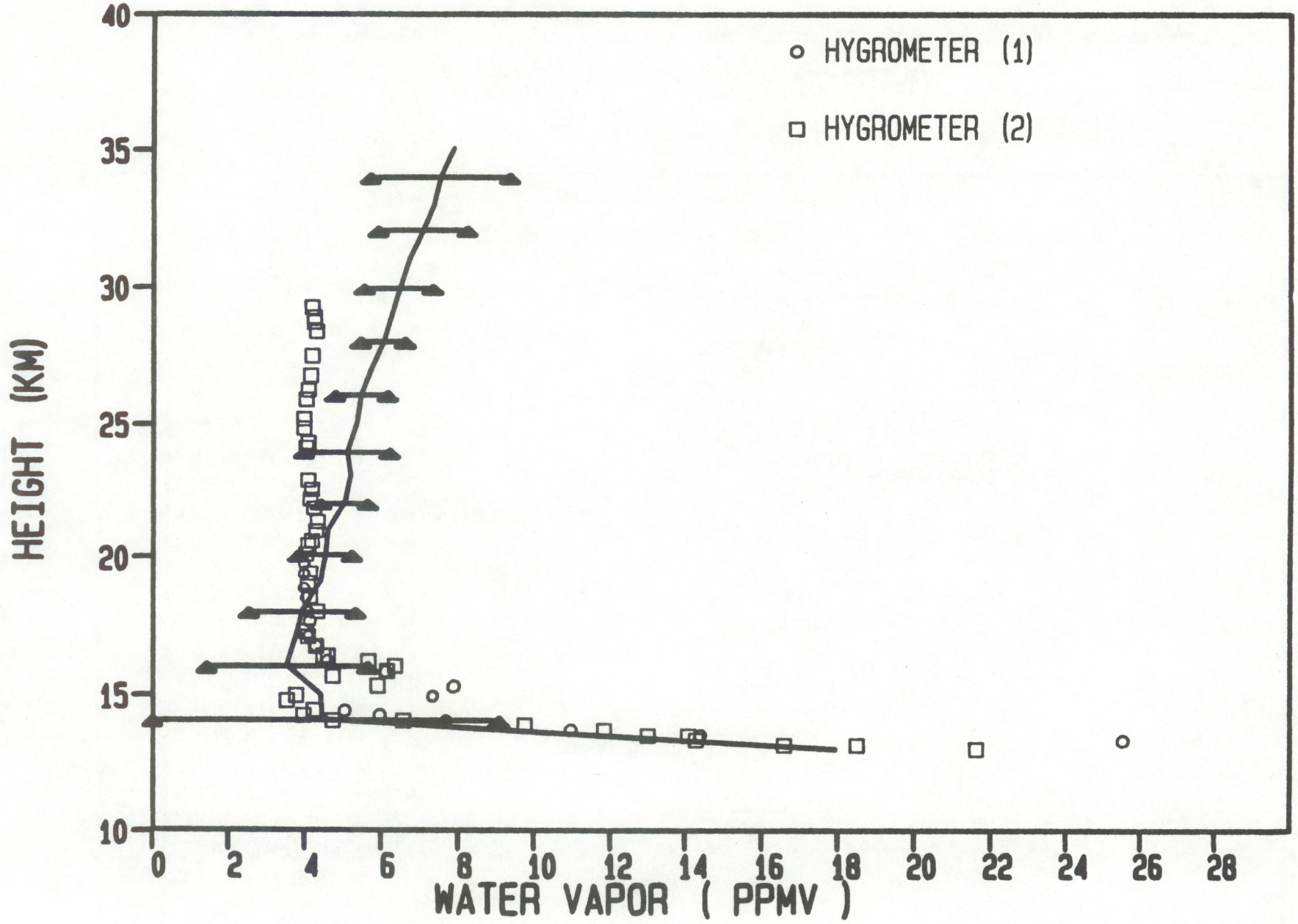

Figure 7. Retrieved water vapor mixing ratio profile and concurrent frost-point hygrometer measurements from 1985 experiment.

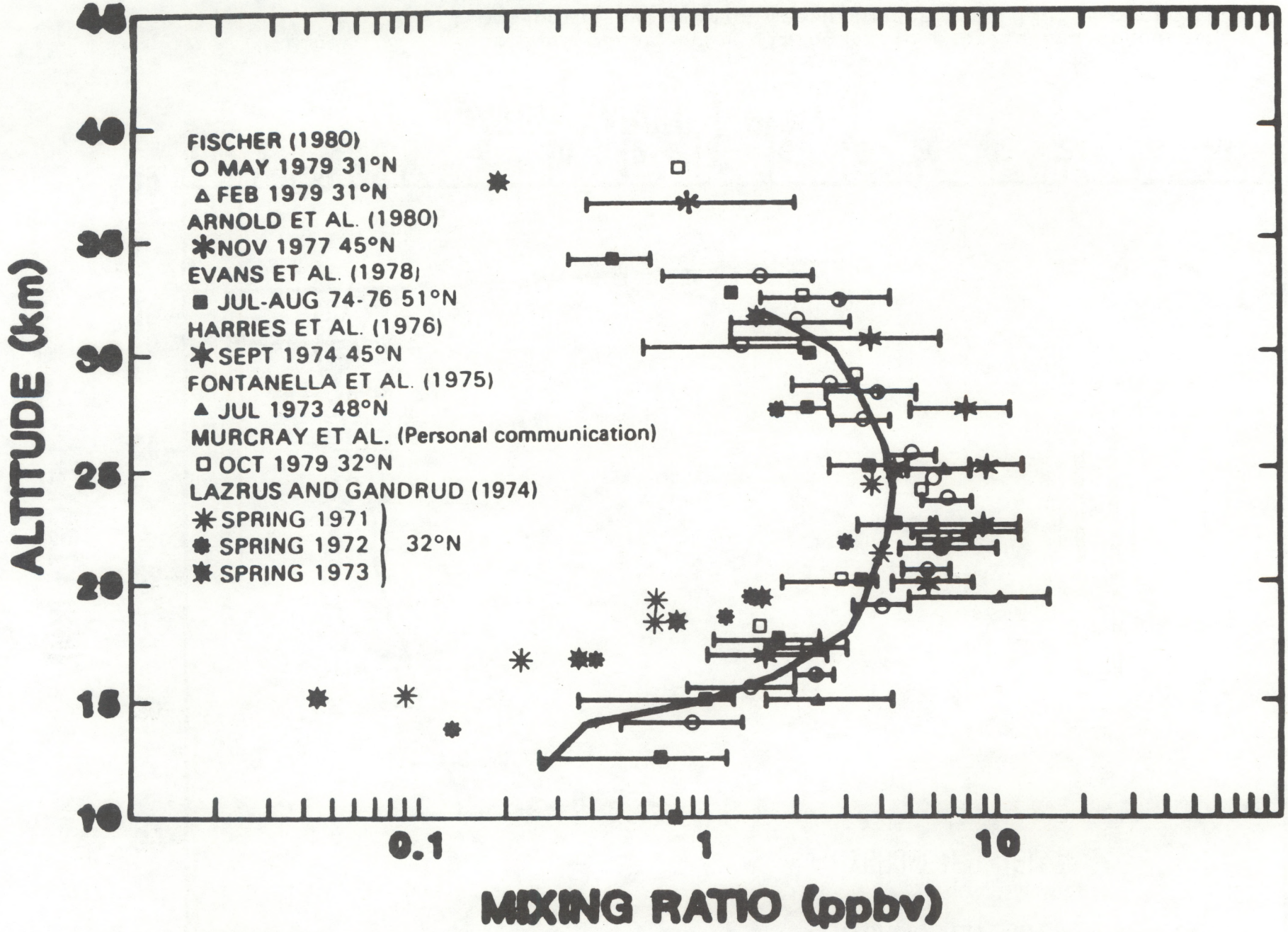

Figure 8. Retrieved nitric acid mixing ratio profile from 1985 experiment superimposed on compilation of previous measurements.

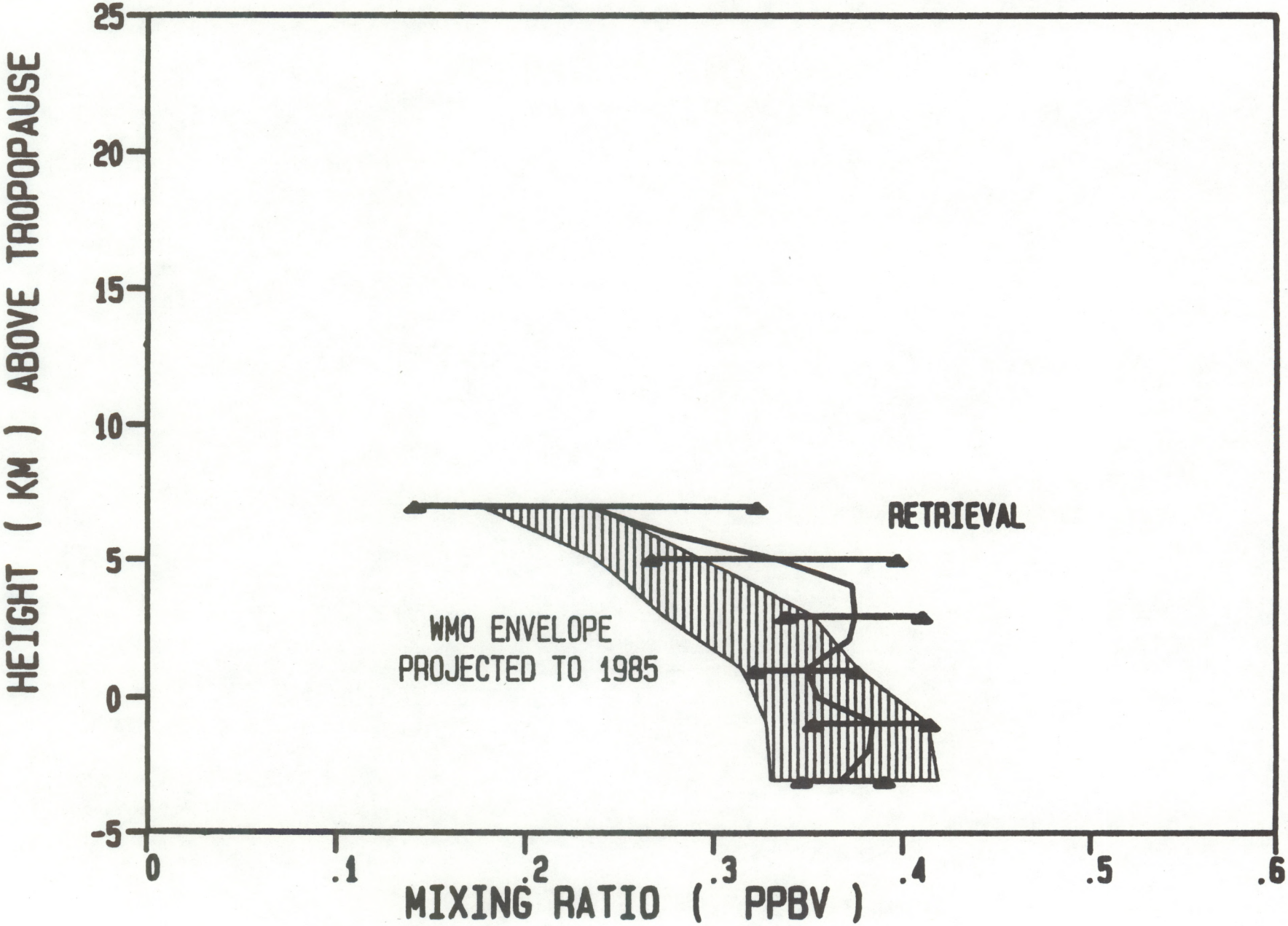

Figure 9. Retrieved Freon-12 mixing ratio profile from 1985 experiments with envelope of prior measurements.

(Continued from inside cover)

NESDIS 6 Spatial and Temporal Distribution of Northern Hemisphere Snow Cover. Burt J. Morse (NESDIS) and Chester F. Ropelewski, October 1983. (PB84 118348)

NESDIS 7 Fire Detection Using the NOAA--Series Satellites. Michael Matson and Stanley R. Schneider (NESDIS), Billie Aldridge and Barry Satchwell (NWS), January 1984. (PB84 176890)

NESDIS 8 Monitoring of Long Waves in the Eastern Equatorial Pacific 1981-83 Using Satellite Multi-Channel Sea Surface Temperature Charts. Richard Legeckis and William Pichel, April 1984. (PB84 190487)

NESDIS 9 The NESDIS-SEL Lear Aircraft Instruments and Data Recording System. Gilbert R. Smith, Kenneth O. Hayes, John S. Knoll, and Robert S. Koyanagi, June 1984. (PB84 219674)

NESDIS 10 Atlas of Reflectance Patterns for Uniform Earth and Cloud Surfaces (NIMBUS-7 ERB--61 Days). V.R. Taylor and L.L. Stowe. (PB85 12440)

NESDIS 11 Tropical Cyclone Intensity Analysis Using Satellite Data. Vernon F. Dvorak, September 1984. (PB85 112951)

NESDIS 12 Utilization of the Polar Platform of NASA's Space Station Program for Operational Earth Observations. John H. McElroy and Stanley R. Schneider, September 1984. (PB85 1525027AS)

NESDIS 13 Summary and Analyses of the NOAA N-ROSS/ERS-1 Environmental Data Development Activity. John W. Sherman III, February 1984. (PB85 222743/43)

NESDIS 14 NOAA N-ROSS/ERS-1 Environmental Data Development (NNEEDD) Activity. John W. Sherman III, February 1985. (PB86 139284 A/S)

NESDIS 15 NOAA N-ROSS/ERS-1 Environmental Data Development (NNEEDD) Products and Services. Franklin E. Kniskern, February 1985. (PB86 213527/AS)

NESDIS 16 Temporal and Spatial Analyses of Civil Marine Satellite Requirements. Nancy J. Hooper and John W. Sherman III, February 1985. (PB86 212123/AS)

NESDIS 17 reserved

NESDIS 18 Earth Observations and The Polar Platform. John H. McElroy and Stanley R. Schneider, January 1985. (PB85 177624/AS)

NESDIS 19 The Space Station Polar Platform: Integrating Research and Operational Missions. John H. McElroy and Stanley R. Schneider, January 1985. (PB85 195279/AS)

NESDIS 20 An Atlas of High Altitude Aircraft Measured Radiance of White Sands, New Mexico, in the 450-1050 nm Band. Gilbert R. Smith, Robert H. Levin and John S. Knoll, April 1985. (PB85 204501/AS)

NESDIS 21 High Altitude Measured Radiance of White Sands, New Mexico, in the 400-2000 nm Band Using a Filter Wedge Spectrometer. Gilbert R. Smith and Robert H. Levin, April 1985. (PB85 206084/AS)

NESDIS 22 The Space Station Polar Platform: NOAA Systems Considerations and Requirements. John H. McElroy and Stanley R. Schneider, June 1985. (PB86109246/AS)

NESDIS 23 The Use of TOMS Data in Evaluating and Improving the Total Ozone from TOVS Measurements. James H. Lienesch and Prabhat K.K. Pandey, July 1985. (PB86108412/AS)

NESDIS 24 Satellite-Derived Moisture Profiles. Andrew Timchalk, April 1986. (PB86 232923/AS)

NESDIS 25 reserved

NESDIS 26 Monthly and Seasonal Mean Outgoing Longwave Radiation and Anomalies. Arnold Gruber, Marylin Varnadore, Phillip A. Arkin, and Jay S. Winston, October 1987. (PB87160545/AS)

NESDIS 27 Estimation of Broadband Planetary Albedo from Operational Narrowband Satellite Measurements. James Wydick, in press.

NESDIS 28 The AVHRR/HIRS Operational Method for Satellite Based Sea Surface Temperature Determination. Charles Walton, in press.

NESDIS 29 The Complementary Roles of Microwave and Infrared Instruments in Atmospheric Sounding. Larry McMillin, in press.

NOAA SCIENTIFIC AND TECHNICAL PUBLICATIONS

The National Oceanic and Atmospheric Administration was established as part of the Department of Commerce on October 3, 1970. The mission responsibilities of NOAA are to assess the socioeconomic impact of natural and technological changes in the environment and to monitor and predict the state of the solid Earth, the oceans and their living resources, the atmosphere, and the space environment of the Earth.

The major components of NOAA regularly produce various types of scientific and technical information in the following kinds of publications:

PROFESSIONAL PAPERS—Important definitive research results, major techniques, and special investigations.

CONTRACT AND GRANT REPORTS—Reports prepared by contractors or grantees under NOAA sponsorship.

ATLAS—Presentation of analyzed data generally in the form of maps showing distribution of rainfall, chemical and physical conditions of oceans and atmosphere, distribution of fishes and marine mammals, ionospheric conditions, etc.

TECHNICAL SERVICE PUBLICATIONS—Reports containing data, observations, instructions, etc. A partial listing includes data serials; prediction and outlook periodicals; technical manuals, training papers, planning reports, and information serials; and miscellaneous technical publications.

TECHNICAL REPORTS—Journal quality with extensive details, mathematical developments, or data listings.

TECHNICAL MEMORANDUMS—Reports of preliminary, partial, or negative research or technology results, interim instructions, and the like.

NATIONAL ENVIRONMENTAL SATELLITE, DATA, AND INFORMATION SERVICE
NATIONAL OCEANIC AND ATMOSPHERIC ADMINISTRATION
U.S. DEPARTMENT OF COMMERCE
Washington, D.C. 20233